Supporting Information

Pulsed-waveform Electrocatalytic Detoxification of Hexavalent Chromium Promoted by Pseudocapacitive Effects

Huaijia Xin [a], *Hang Wang* [c], *Wei Zhang* [a], *Yang Liu* [a], *Jun Zhang* [a], *Gong Zhang* [a], *Qinghua Ji* [a*], *Huijuan Liu* [a], *Jiuhui Qu* [a,b]

[a] Center for Water and Ecology, State Key Joint Laboratory of Environment Simulation and Pollution Control, School of Environment, Tsinghua University, Beijing 100084, China

[b] Key Laboratory of Drinking Water Science and Technology Research Centre for Eco-Environmental Sciences, Chinese Academy of Sciences, Beijing 100085, China

[c] Department of Chemical and Biomolecular Engineering, Tandon School of Engineering, New York University, New York 11201, USA

[*] Corresponding Author:

E-mail: qhji@tsinghua.edu.cn; Phone: (8610)6279-0565; Fax: (8610)6292-3558.

This file contains: 14 pages; 17 figures.

■ Experimental Section

Preparation of Carbon-based Electrodes. Carbon paper and the activated carbon power were supplied by Toray Industries, Inc and Shanghai Jiuding Chemical Technology Co., Ltd, respectively. The carbon paper electrode (2 × 2 cm^2) was prepared by hydrothermally treating in HNO_3 solution at 80°C for 2 h to obtain hydrophilic substrates. The activated carbon electrode was prepared by sticking the activated carbon powder (0.2 mg) onto the ITO substrate (2 × 2 cm^2) with naphthol solution.

Preparation of the Flow-through PANI Electrode. The PANI was obtained by flow-through electrodeposition of aniline monomer on the 316L SS. The electrolyte was composed of 0.5 M aniline and 1 M $HClO_4$. Typically, IrTa electrodes were used as anode while 316L SS were used as cathode, which were separated by a porous insulating spacer. Ten pairs of SS and IrTa were staked in a single flow-through cell, and the electrolyte was injected into the anodic end of the cell and flow through the SS electrodes at a flow rate of 150 L/h/m^2 and finally out of the cell. The flow-through electrodeposition was carried out with a cell voltage of 1.8 V for 600 s. After polymerization, the as-prepared PANI electrodes were taken out and washed with the ultrapure water. Finally, the PANI electrode were freeze-dried for further application (Figure S16).

Fabrication of the Flow-through Cell. PANI supported on the SS (4 × 5 cm^2) and the commercial iridium tantalum modified titanium mesh (IrTa, 4 × 5 cm^2) were used as the cathode and anode, respectively. Ten pairs of cathodes and anodes separated by porous insulating spacer were stacked and loaded into a flow-through cell (denoted as

the PANI/IrTa flow-through cell) (Figure 6a). Each pair of PANI and IrTa electrodes were connected in series. Stainless steel wires were used to connect all the PANI and IrTa, respectively, and then connected to the corresponding cathode and anode of the power supply.

Flow-through Experiments. All experiments were conducted in a two-electrode system with 10 ppm Cr(VI) (pH = 2). The influent was injected into the PANI/IrTa flow-through cell through an inlet by a peristaltic pump and the effluent was discharged through an outlet by a peristaltic pump as well. The retention time was 5 min or 10 min. Comparisons between the constant and pulsed voltages on the reduction efficiency of Cr(VI) were carried out with the cell voltages ranging from 1.0 to 1.6 V. The durability of the PANI flow-through electrode in electrocatalytic reduction of Cr(VI) under the pulsed voltage was also evaluated.

■ Results and Discussion

Characterization of the PANI Electrode. The XPS widerange spectra show that the N content of PANI film and PANI nanoarray were 8.1% and 7.4%, respectively (Figure S3a). High-resolution N 1s spectra demonstrate that the N functional groups were divided into three fitted peaks centered at 398.3, 399.9 and 401.9 eV, which represent the quinoid amine (=N−), benzenoid amine (−NH−), and the nitrogen cationic radical (N+·), respectively (Figure S3b).[1, 2] The area fraction of the protonated nitrogen atoms indicates the doping level of the PANI film and PANI nanoarray were 15.7% and 8.3%, respectively. In the FT-IR spectra, four typical bands corresponding to the PANI

appeared at 1143, 1307, 1495 and 1581 cm^{-1}, corresponding to the aromatic C–H in-plane bending, C–N stretching of secondary aromatic amine, and the C=C stretching vibrations of benzenoid and quinoid ring structure (Figure S3c).[1-3] The relative strength of peak intensities between quinoid ring (1581 cm^{-1}) and benzenoid ring (1495 cm^{-1}) was related to the extent of oxidation,[2] and the relative absorption intensities at 1142.7 cm^{-1} corresponded to the extent of protonation,[4] which were similar both in the PANI film and PANI nanoarray. Complementary structure information was provided by Raman spectra (Figure S3d), which were detailed describe in the section of *in situ* Raman Spectroscopy.

In situ Raman Spectroscopy Confirmed that PANI Reduced Cr(VI) during the Off-voltage Time

The oxidation reactions associated with LB/ES and ES/PB conversions:

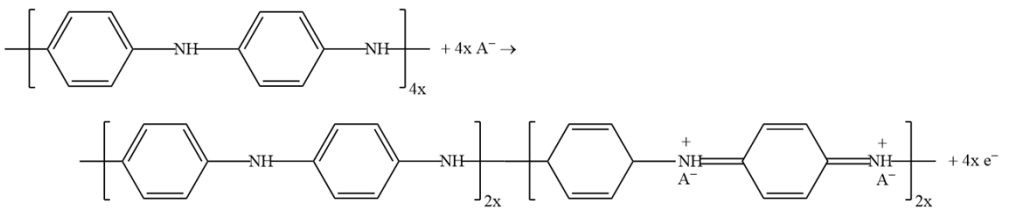

(1)

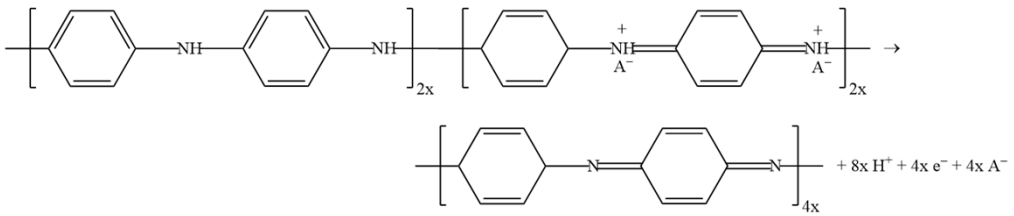

(2)

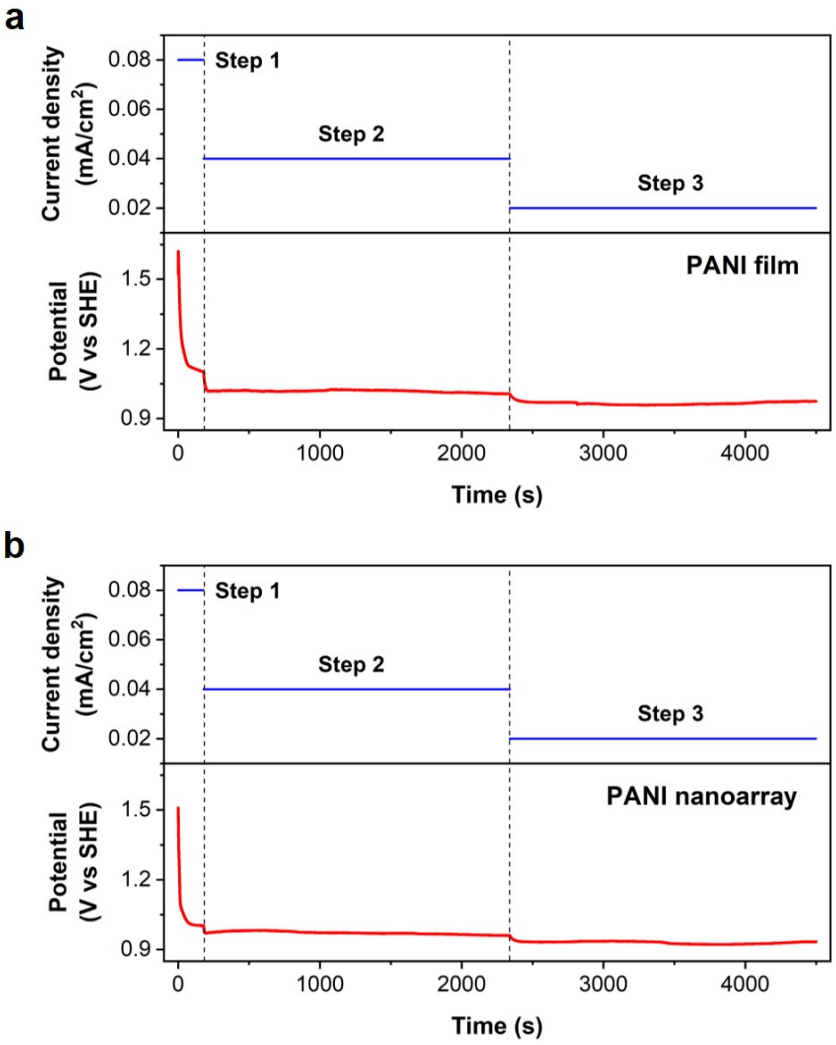

Figure S1. The potential variation during the galvanostatic procedure for the electrodeposition of (a) PANI film and (b) PANI nanoarray supported on ITO substrates

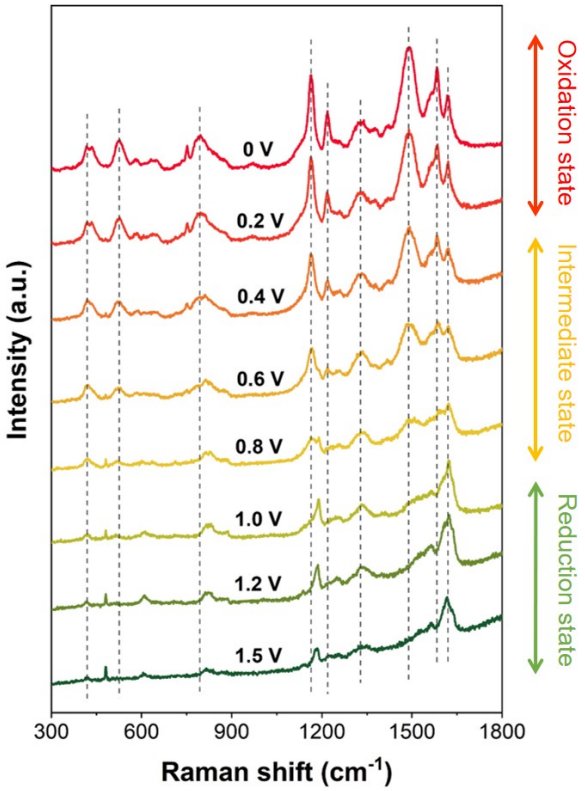

Figure S2. Raman spectra of PANI in 10 ppm Cr(VI) at different constant voltages.

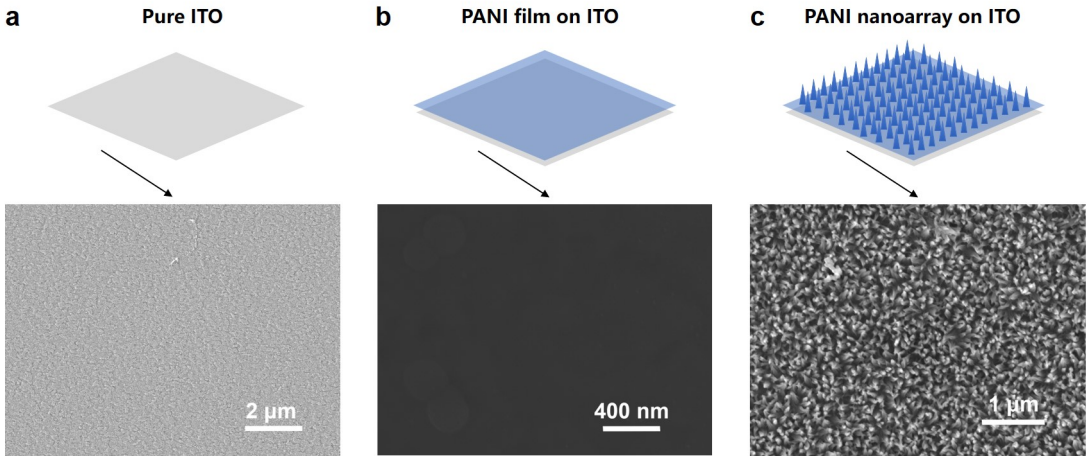

Figure S3. SEM images of (a) ITO substrate, (b) PANI film and (c) PANI nanoarray supported on the ITO.

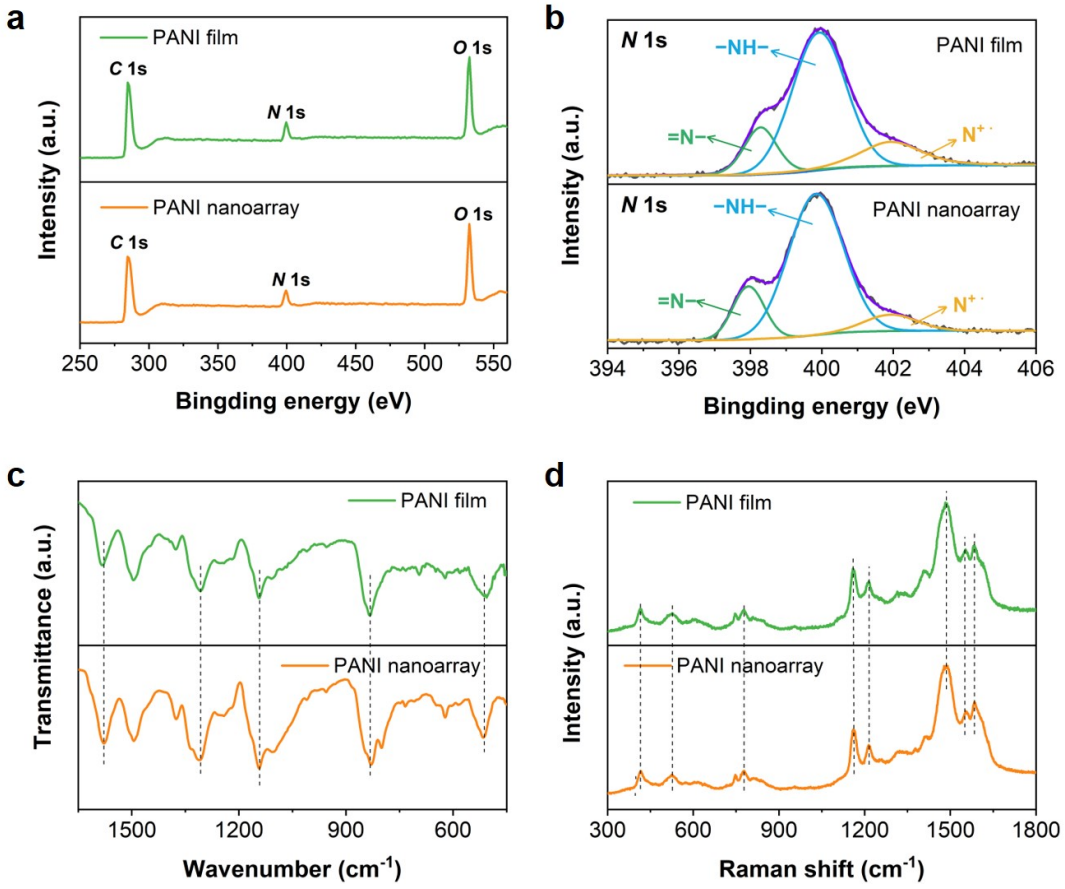

Figure S4. PANI electrode characterization. (a) XPS (b) XPS *N* 1s, (c) FT-IR, and (f) Raman spectra.

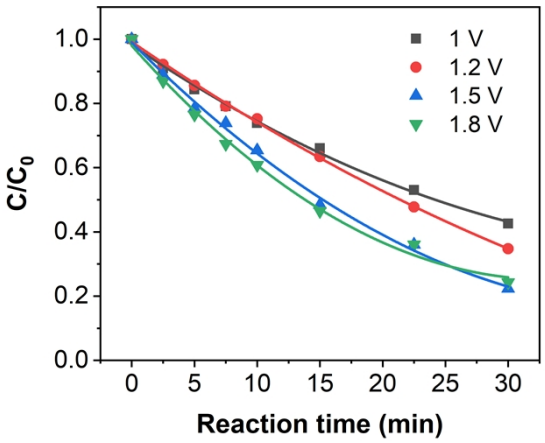

Figure S5. Effect of cell voltages on Cr(VI) reduction. Experiments were conducted at various pulsed voltages (0.2 Hz, $t_{on} = t_{off}$). Initial [Cr(VI)] = 10 ppm and pH = 2.

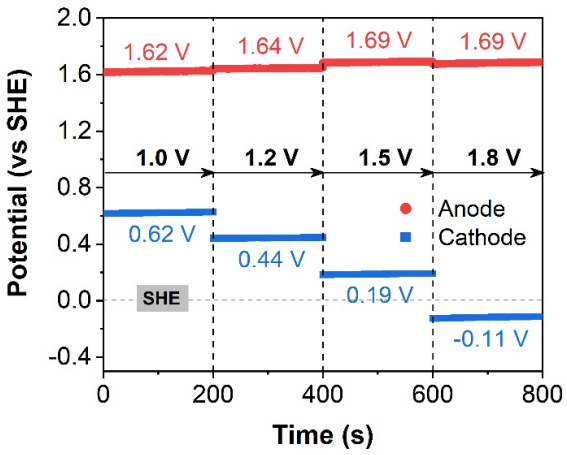

Figure S6. The anode and cathode potentials at different cell voltages. Initial [Cr(VI)] = 10 ppm and pH = 2. SHE: standard hydrogen electrode.

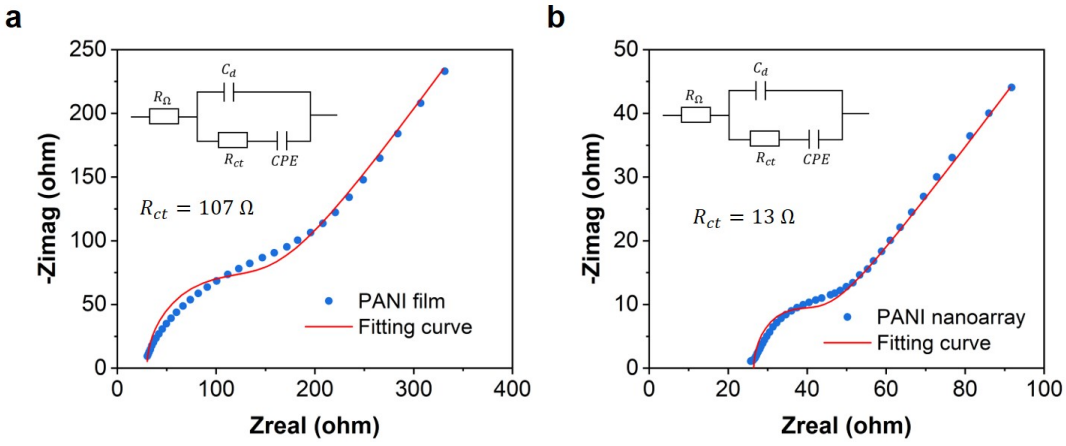

Figure S7. EIS curves for (a) PANI film and (b) PANI nanoarray.

Table S1. Parameters of the electrical equivalent circuit of EIS analysis

Electrode	R_Ω (Ohm)	C_d (F)	R_{ct} (Ohm)	Q (F·s^(α-1))	ω (°)	α (1)
PANI film	30	2.9×10^{-7}	107	1.35×10^{-4}	47.7	0.53
PANI nanoarray	26.5	2.4×10^{-5}	13	6.5×10^{-3}	39.6	0.44

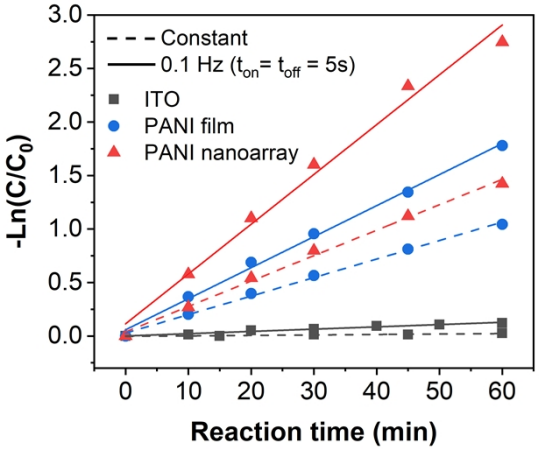

Figure S8. Kinetics investigation of Cr(VI) reduction with different cathodes at the constant and pulsed voltages of 1.5 V. Initial [Cr(VI)] = 10 ppm and pH = 2.

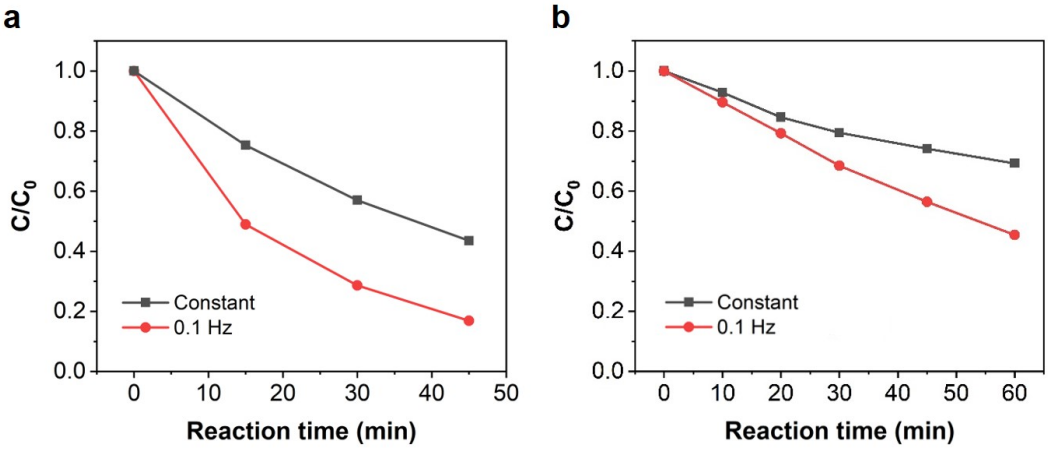

Figure S9. Cr(VI) reduction efficiency at the constant and pulsed voltages of 1.5 V: (a) carbon paper electrode and (b) activated carbon electrode. Initial [Cr(VI)] = 10 ppm and pH = 2.

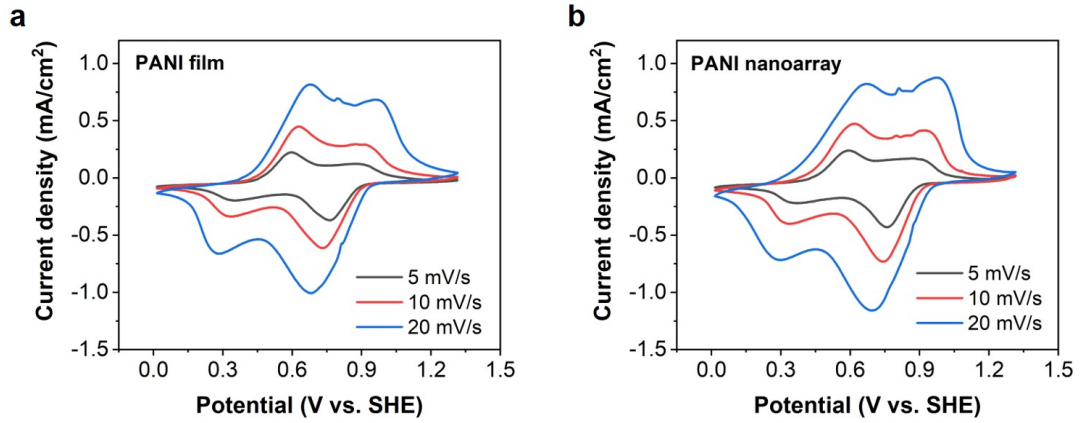

Figure S10. Cyclic voltammetry at different scan rates: (a) PANI film and (b) PANI nanoarray.

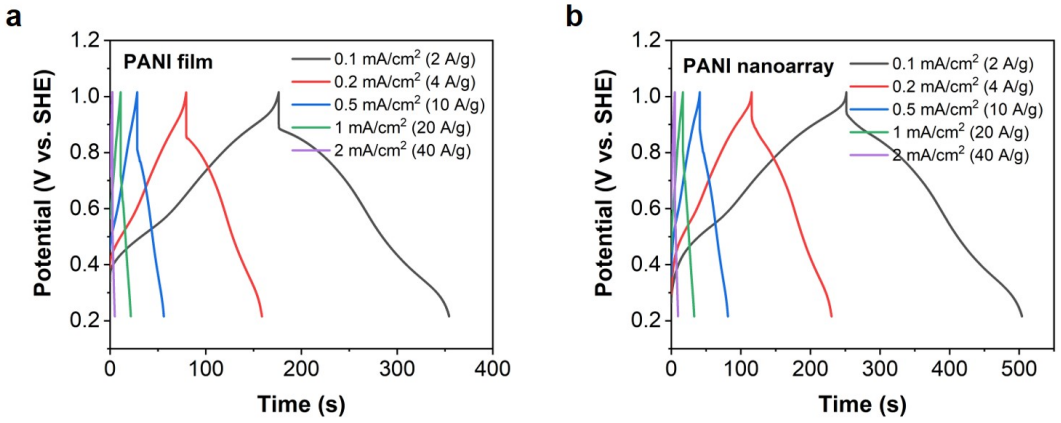

Figure S11. Typical galvanostatic charge–discharge curves at several current densities: (a) PANI film and (b) PANI nanoarray.

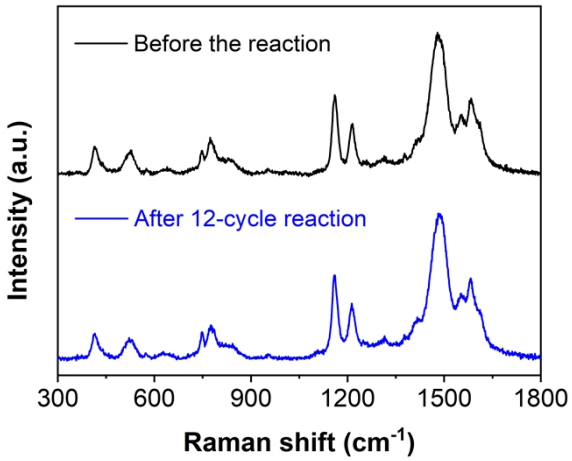

Figure S12. Raman spectra of the PANI nanoarray before and after 12-cycle reaction.

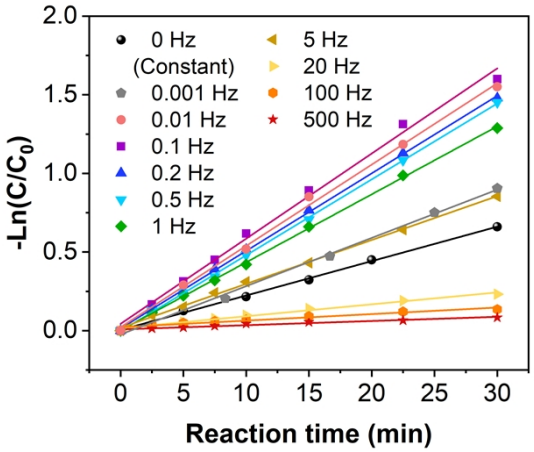

Figure S13. Kinetics investigation of Cr(VI) reduction at a pulsed voltage of 1.5 V with the frequencies of 0 (constant) to 500 Hz and the on-off ratio of 50%. The PANI nanoarray served as the cathode. Initial [Cr(VI)] = 10 ppm and pH = 2.

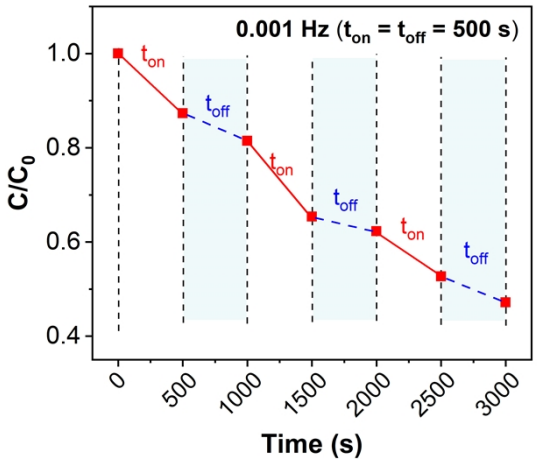

Figure S14. Cr(VI) reduction efficiency at t_{on} and t_{off} under 0.001 Hz pulsed voltage of 1.5 V. Initial [Cr(VI)] = 10 ppm and pH = 2.

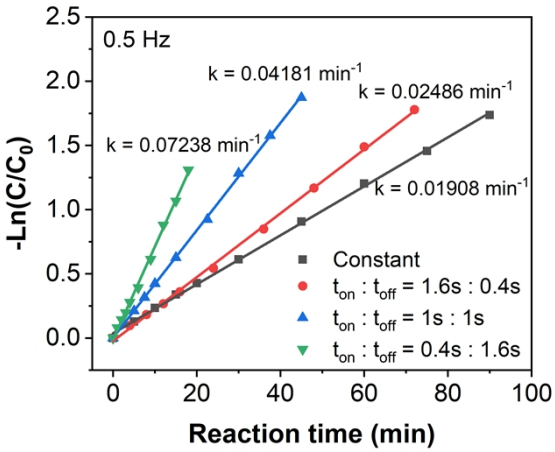

Figure S15. Influence of the on-off ratios on Cr(VI) reduction kinetics at the pulsed voltage of 1.5 V with the frequency of 0.2 Hz. The PANI nanoarray served as the cathode. Initial [Cr(VI)] = 10 ppm and pH = 2.

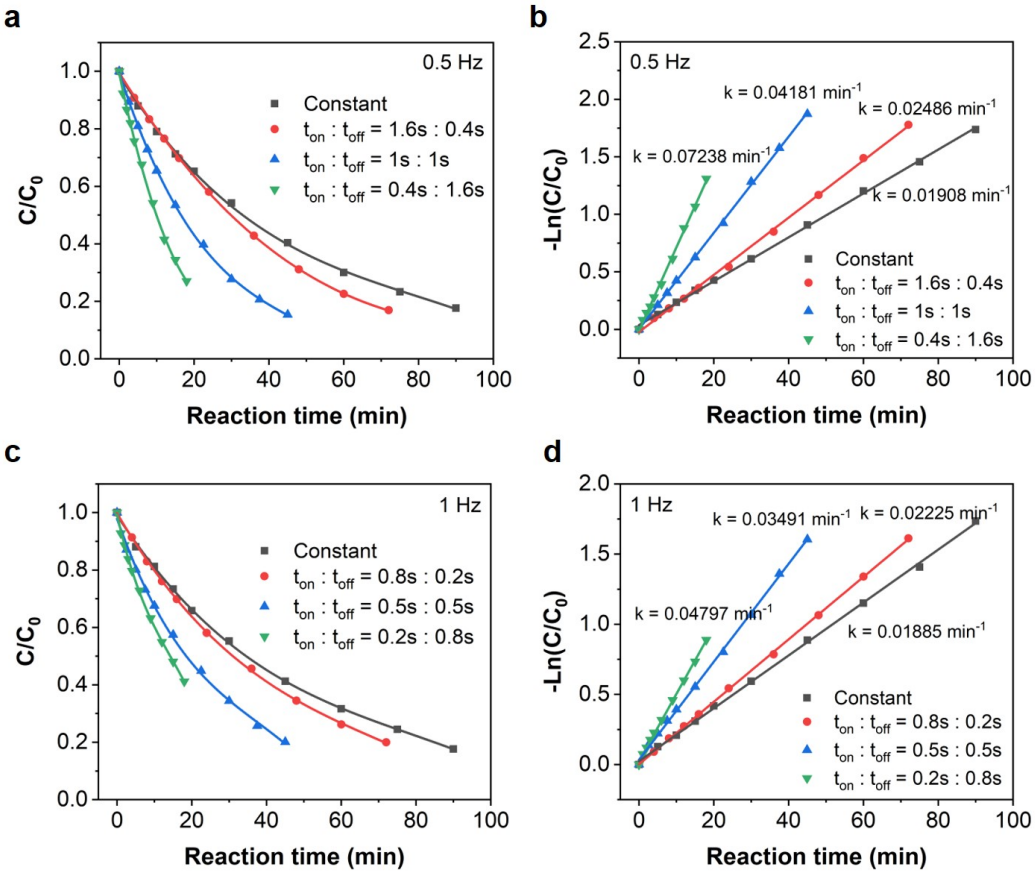

141

142 **Figure S16.** Influence of the on-off ratios on Cr(VI) reduction kinetics at the pulsed

143 voltage of 1.5 V with the frequency of (a–b) 0.5 Hz and (c–d) 1 Hz. The PANI

144 nanoarray served as the cathode. Initial [Cr(VI)] = 10 ppm and pH = 2.

145

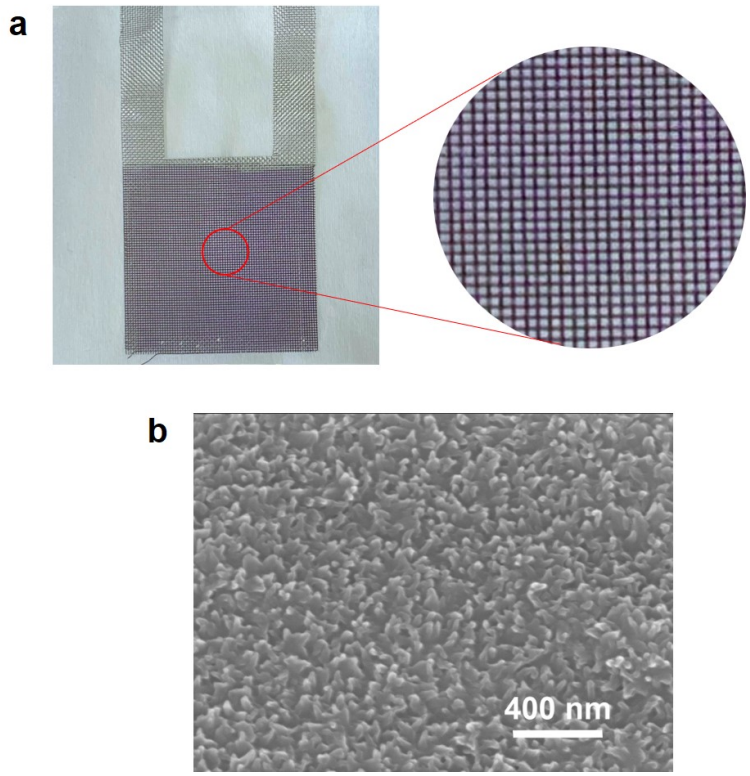

Figure S17. (a) Photograph and (b) SEM images of the PANI supported on the SS.

References

1. Y. Yang, M. h. Diao, M. m. Gao, X. f. Sun, X. w. Liu, G. h. Zhang, Z. Qi and S. g. Wang, *Electrochimica Acta*, 2014, **132**, 496-503.
2. Z. Tong, Y. Yang, J. Wang, J. Zhao, B.-L. Su and Y. Li, *J. Mater. Chem. A*, 2014, **2**, 4642-4651.
3. X. Xiong, Q. Qiao, Q. Zhou, X. Cheng, L. Liu, L. Fu, Y. Chen, B. Wang, X. Wu and Y. Wu, *Nano Research*, 2023, DOI: 10.1007/s12274-022-5370-7.
4. H. V. Dias, X. Wang, R. M. Rajapakse and R. L. Elsenbaumer, *Chem. Commun.*, 2006, DOI: 10.1039/b513938d, 976-978.